



Observations of a systematic selected sample of X-ray bright HBL objects with the MAGIC telescope

M. MEYER¹, T. BRETZ¹, D. DORNER¹, E. PRANDINI², ON BEHALF OF THE MAGIC COLLABORATION

¹*Institut für Theoretische Physik und Astrophysik, Univ. Würzburg, D-97074 Würzburg, Germany*

²*Dipartimento Di Fisica G. Galilei, Univ. di Padova, (35100) Padova, Italy*

meyer@astro.uni-wuerzburg.de

Abstract: Up to now, nearly all the detected extragalactic VHE gamma-ray sources belong to the class of high-frequency peaked BL Lac objects (HBL), which show a pronounced peak in the X-ray band.

MAGIC has started a systematic scan on X-ray bright HBL objects in the northern sky during its cycle 1 observations from January 2005 to March 2006. Following the blazar compilation by Donato et al. (2001), 13 HBLs were selected with the criteria of low redshift ($z < 0.3$), high X-ray flux ($F(1 \text{ keV}) > 2 \mu\text{Jy}$) and visibility under small zenith distances ($z_d < 30^\circ$ at culmination, leading to sources with a declination between -2° and $+58^\circ$).

In that campaign IES 1218+30.4 was discovered and IES 2344+51.4 was detected in a low flux state with high significance. Here the 99% confidence level upper limits on the integral flux above $\sim 200 \text{ GeV}$ for ten sources are presented as well as the results of an observation of IES 1218+30.4 from January to March 2007. The analysis yields a marginal detection of 4.4σ , corresponding to an integral flux above 180 GeV of $F = (1.46 \pm 0.48) \times 10^{-11} \text{ photons cm}^{-2}\text{s}^{-1}$, which is $\sim 40\%$ lower than the flux measured in January 2005. The absorption corrected upper limits for the luminosities at 200 GeV are compared to archival X-ray data and discussed with respect to established TeV sources.

Introduction

Despite the recently discovered BL Lacertae as well as the giant radio galaxy M87, all extragalactic VHE sources belong to the sub-class of HBLs. Due to the small field-of-view of an Imaging Air Cherenkov Telescope (IACT) and a duty cycle of ~ 1000 hrs per year, the selection of promising candidates for VHE emission becomes important in the search for new VHE sources. All established TeV sources are bright X-ray sources, most of them with comparable luminosities in both regimes, which makes a systematic search for the brightest X-ray HBL objects reasonable.

HBL sample

The compilation from [1], which provides radio, optical and X-ray data for 136 HBL objects was used. The selection criteria were (i) redshift $z < 0.3$, (ii) X-ray flux $F_x(1 \text{ keV}) > 2 \mu\text{Jy}$, and zenith distance $z_d < 30^\circ$ during culmination. At $z = 0.3$,

the expected cut-off energy due to absorption in the metagalactic radiation field (MRF) is still above 200 GeV , where MAGIC has its highest sensitivity. As the energy threshold increases with the zenith distance, all observations were done below 40° . Only the X-ray brightest HBL were selected, leading to a cut at $2 \mu\text{Jy}$. Assuming the same luminosity at $\sim 200 \text{ GeV}$ (which is the case for half of all HBLs detected at VHE), it corresponds to $\sim 7\%$ of the flux of the Crab Nebula.

The selected targets are listed in Table 1. In addition also Mrk 421, Mrk 501 and IES 2344+51.4 fulfill the selection criteria (see [2], [3] and [4] respectively).

Observations

The MAGIC telescope is a single dish IACT, located on the Canary island of La Palma (28.8°N , 17.8°W , 2200 m a.s.l.). A parabolic mirror with a total surface of 234 m^2 focuses Cherenkov light from air showers onto a 576 -pixel photomultiplier

(PMT) camera with a field-of-view of 3.5° . Further details on the telescope can be found in [5].

The observations took place from January 2005 to March 2006. The data were taken in different observation modes. If the telescope is pointing to the source (on-mode), the background has to be determined by so-called off-data, where the telescope points to a sky region where no gamma-ray source is expected. The larger fraction of the source sample was observed in the so-called wobble mode, where the telescope is pointing 0.4° away from the source. The position is changing every 20 minutes to the opposite to achieve a symmetric coverage in the camera.

Despite 1ES 0927+50.0 and 1ES 0414+00.9, all objects were monitored by the KVA telescope (<http://tur3.tur.iac.es/>) on La Palma in the optical range. The simultaneous taken, host galaxy corrected fluxes are listed in Table 1.

Data analysis technique

The data were processed using the MAGIC Analysis and Reconstruction Software (MARS) [6]. A description of the different analysis steps can be found in [7] (including the calibration) and [8]. The gamma-hadron separation used here is described in [9]. The cut coefficients for the background suppression were optimised using data of the Crab Nebula. One set of cut coefficients was derived for data taken in on-off mode and one for wobble mode. For wobble observations, three regions located symmetrically on a ring around the camera centre with the same distance from the centre as the source position, were defined as background regions.

The statistical significance is calculated according to equation 17 in [10]. The upper limit on the excess rate is derived with a confidence level (c.l.) of 99%, using the method from [11], which takes also the scaling factor of the background into account. The upper limit for the excess rate is then compared to the excess rate of the Crab Nebula, which leads to a flux upper limit in units of the Crab Nebula flux above a certain threshold, assuming a Crab like spectrum. The energy threshold here is defined as the peak energy of simulated gamma-rays, surviving all cuts. Note that this threshold depends

also on the spectrum. The Crab units are converted into a flux of photons $\text{cm}^{-2} \text{s}^{-1}$ using the spectrum of the Crab Nebula from [12].

The systematic error for the flux is dominated by the error of the Crab Nebula flux, which is estimated to be $\sim 30\%$ (see [12] and discussion therein). In addition for the u.l. determination there are the uncertainties of the reference excess rate of Crab as well as of the correct energy threshold (which depends on the source spectrum).

Results

The u.l. lie between 2.3% and 8.6% of the Crab Nebula flux at energy thresholds between 190 GeV and 230 GeV (for a Crab like spectrum), depending on the zd of the observation (see Table 1). As the Crab spectrum at ~ 200 GeV is quite hard (spectral slope -2.3 for the differential energy spectrum), the u.l.s are also calculated for an -3.0 power law spectrum, which represents quite well the average slope of all HBLs detected at VHE so far.

1ES 1218+30.4 was observed in 2006 from January the 29th to March the 5th in 15 nights with 14.6 hrs in total. Figure 1 shows the distribution of the squared angular distance between the reconstructed shower origin of each event and the assumed source position. The vertical line indicates the signal region, which contains 378 excess events over 5456 background events (scaled by 0.33) corresponding to a statistical significance of 4.4σ .

Under the assumption of a power law spectrum with spectral slope of -3.0 as measured in 2005 [9], the peak response energy lies at 190 GeV. The average integral flux above 180 GeV for the complete sample is $F(> 180 \text{ GeV}) = (1.46 \pm 0.48) \times 10^{-11} \text{ photons cm}^{-2} \text{ s}^{-1}$, which is $\sim 40\%$ less than in January 2005.

Discussion

All u.l.s at 200 GeV as well as the fluxes of the detected TeV sources are corrected for the absorption, using the "best fit 2006" MRF-model from [13]. This model is based on the "best fit" model from [14], but with a lower star formation rate, to keep the energy density in the optical band consistent with the u.l. derived by [15].

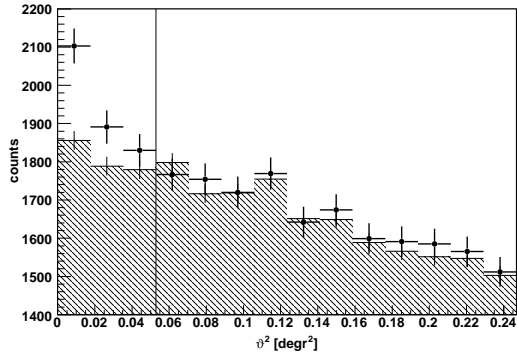


Figure 1: Distribution of ϑ^2 with respect to the position of 1ES 1218+30.4 (dots).

Figure 2 shows the overall spectral index $\alpha_{X\gamma}$ ($= -\log(F_X(1 \text{ keV})/F_\gamma(200 \text{ GeV})/\log(\nu_X/\nu_\gamma))$) vs. X-ray luminosity $\nu_X L_X$ at 1 keV^1 . The average X-ray flux never exceeds significantly the flux at 200 GeV. For half of the detected sources, the fluxes in these energy bands are almost the same, while for the other ones the gamma-ray flux is significant lower. There is at least the hint, that this effect show up at higher luminosities. For the non-detected sources of the sample, further observations with longer exposures are needed to reach the $\alpha_{X\gamma} = 1.10$ -line, which includes all HBLs detected at VHE so far.

Acknowledgements

We would like to thank the IAC as well as the German BMBF and MPG, the Italian INFN and the Spanish CICYT. This work was also supported by ETH Research Grant TH 34/04 3 and the Polish MNI Grant 1P03D01028.

References

- [1] D. Donato, G. Ghisellini, G. Tagliaferri, G. Fossati, *A&A* 375 (2001) 739.
- [2] J. Albert, E. Aliu, H. Anderhub, et al., *ApJ* 663 (2007) 125.
- [3] J. Albert, E. Aliu, H. Anderhub, et al., accepted by *ApJ*, arXiv:astro-ph/0702008.

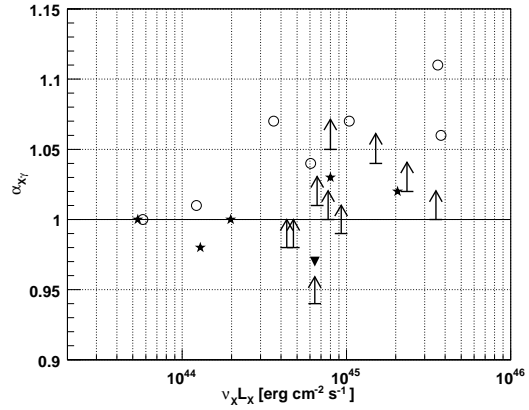


Figure 2: The overall spectral index $\alpha_{X\gamma}$ vs. the X-ray luminosity $\nu_X L_X$. The arrows mark the u.l.s. calculated in this work, while the stars indicate the detected sources that belong to the sample and the open circles mark all other detected HBLs.

- [4] J. Albert, E. Aliu, H. Anderhub, et al., *ApJ* 662 (2007) 892.
- [5] C. Baixeras, D. Bastieri, C. Bigongiari, et al., *Nucl. Instr. and Meth. A* 518 (2004) 188–192.
- [6] T. Bretz, in: in *AIP Conf. Proc.* 745, 2005, p. 730.
- [7] M. Gaug, H. Bartko, J. Cortina, J. Rico, in: *Proc. of the 29th Int. Cosmic Ray Conf. (Pune)*, 5, 2005, p. 375.
- [8] T. Bretz, in: *Proc. of the 29th Int. Cosmic Ray Conf. (Pune)*, 4, 2005, p. 315.
- [9] J. Albert, E. Aliu, H. Anderhub, et al., *ApJL* 642 (2006) L119–L122.
- [10] T. Li, Y. Ma, *ApJ* 272 (1983) 317.
- [11] W. A. Rolke, A. M. López, J. Conrad, *Nucl. Instr. and Meth. A* 551 (2005) 493–503.
- [12] J. Albert, E. Aliu, H. Anderhub, et al., submitted to *ApJ*, arXiv:0705.3244v1 [astro-ph].
- [13] T. M. Kneiske, in preparation.
- [14] T. M. Kneiske, T. Bretz, K. Mannheim, D. Hartmann, *A&A* 413 (2004) 807.
- [15] F. Aharonian, A. G. Akhperjanian, A. R. Bazer-Bachi, et al., *Nature* 440 (2006) 1018.

1. The X-ray fluxes are the average from [1]

(1) Source	(2) z	(3) Mode	(4) Exp. [hrs]	(5) Zd degr.	(6) E_{thres} GeV	(7) Excess	(8) Back.	(9) scale	(10) S
1ES 0120+34.0	0.272	w	14.9	12.2	190	-48	5358	0.33	-0.1
RX J0319.8+1845	0.190	w	4.7	14.3	190	9	2225	0.33	0.0
RX J0319.8+1845	0.190	on	6.5	14.2	190	-95	3257	0.86	-0.1
1ES 0323+02.2	0.147	w	11.4	29.0	230	55	5262	0.33	0.0
1ES 0414+00.9	0.287	w	17.8	29.7	230	176	7309	0.33	1.0
1ES 0806+52.4	0.138	w	17.5	26.8	230	111	6174	0.33	1.0
1ES 0927+50.0	0.188	w	16.1	22.1	230	72	5721	0.33	0.0
1ES 1011+49.6	0.200	w	14.5	23.6	230	200	4857	0.33	2.0
1ES 1218+30.4	0.182	w	14.6	26.6	230	378	5456	0.33	4.0
RX J1417.9+2543	0.237	on	13.0	9.7	190	-137	9007	1.03	-0.1
1ES 1426+42.8	0.129	on	6.1	16.6	190	-7	2561	0.24	-0.1
RX J1725.0+1152	>0.17	on	5.3	17.4	190	-69	2001	0.98	-0.1

Table 1: Systematic selected sample of X-ray bright HBL objects. Columns: (1) : object name or on-off mode (on); (4) : observation time after quality selection [hrs.]; (5) : mean zenith di like spectrum; (7) : number of excess events; (8) : number of background events (after scaling wobble mode); (10) : statistical significance following equation 17 from [10]; (11) : upper limit (c.u.) for a 99% confidence level and a Crab like spectrum; (12) : flux u.l. in flux units (f.u. = 1 for a -3.0 power law spectrum); (14) : u.l. for the flux at 200 GeV in units of 10^{-12} erg cm^{-2} s^{-1} ; 1218+30.4 the flux at 200 GeV is given; (15) : host galaxy corrected simultaneous optical flux 10^{-12} erg cm^{-2} s^{-1}